Acknowledgements

I would like to thank my co-supervisor Iver Bakken Sperstad at SINTEF Energi for answering my questions, useful discussions regarding the thesis and general guidance. I would also like to thank Assoc. Prof. Jon Andreas Støvneng for agreeing to be my supervisor. Finally, I want to thank Henrik for our fruitful discussions and Annagha for her support.

Sammendrag

I denne masteroppgaven er kraftsystemet studert ved bruke det kanoniske ensemblet fra statistisk mekanikk. Relativt nye fremskritt lar oss inkludere dynamikken i kontinuerlige tilstandsvariabler som modellerer av/på status i transmisjonsliner i et system styrt svingeligningen. Det viser seg at denne modellen kan beskrives av en Hamiltonian-aktig energifunksjon. Ved bruke energifunksjonen kan vi evaluere systemet fra et energetisk synspunkt, noe som muliggjr bruken av det kanoniske ensemblet. Noen av resultatene er enkle tolke og gir mening, mens andre ikke. Endringer i energifunksjonen som fasiliterer arbeidet fra et energetisk standpunkt er foreslått og utprøvd. Resultaten av arbeidet er positive, men gir ikke grunnlag for konkludere om en statistisk mekanisk tilnrming er nyttig eller ei.

Abstract

In this thesis the power system is studied using the canonical ensemble from statistical mechanics. Relatively new developments allow us to include in a swing equation model the dynamics of continuous state variables modeling the on-off status of transmission lines. It turns out that this model can be described by a Hamiltonian-like energy function. Using the energy function we can evaluate the system from an energetic viewpoint, making the application of the canonical ensemble possible. Some of the results give clear meaning and are easily interpreted, while other parts less so. Changes to the energy function to make it easier to work with from an energetic viewpoint are proposed and tested. The results of this work are positive, but inconclusive in determining the usefulness of a statistical mechanical approach.

Table of Contents

Chapter 1

Introduction

Large blackouts or cascading outages are events in the electrical power system that have a very small probability of occurring but very serious societal consequences if they do. For this reason, such events are also referred to as high-impact low-probability (HILP) events or extraordinary events. Understanding and identifying such events has proven to be a great challenge that defeats conventional methods of power system analysis. Such problems are challenging because cascading outages involve a large and diverse number of complex phenomena.Furthermore, power transmission systems consist of thousands of components, adding another layer of complexity.

This problem has attracted interest from the physics community. The approaches used can be divided into two groups. The first being complex network modeling of the power system, which relies on purely topological measures of the network quality (however one wants to define it), and which has been quite extensively investigated [1, 2]. These approaches usually include quasi static modeling of power flows, disregarding the dynamic nature of the power system, and it follows that they are limited in the amount of insight they can provide.

However, dynamic modeling of the power system [3–6], gives a more detailed description of the system than the complex network approach. This set of approaches can be made arbitrarily complex to the point where a physicist would be better off leaving the job to an electrical engineer. There are, however, opportunities to consider simpler models which might lend themselves to be studied with tools from the physicist's toolbox.

Apart from this there seems to be no statistical mechanical approaches using power grid models. General complex networks have been studied using statistical mechanics e.g. [7–9] but this has not been done with complex network models of the power system, much less with more detailed power system models. This is then pretty much uncharted territory which is an interesting point of departure for a master's thesis.

As mentioned, the power system consists of many components. Each of these components can be considered as moving parts of a mechanical system. This encompasses the physically moving parts such as generators, as well as parts that can be represented by moving state variables such as the on/off status of a transmission line. Depending on how the power system is modeled, the behavior of all its moving parts may be determined from a set of initial conditions. However, as alluded to earlier, the number of different initial conditions and moving parts one would have to consider to be able to make a statement about the systems stability is potentially enormous. This is a problem that has already been encountered in several areas of physics. Examples include determining the thermodynamic properties of a gas of particles or magnetic spins on a lattice.

The act of connecting knowledge of the systems microscopic behavior (the equations of motion of its moving parts) to its macroscopic behavior (the collective behavior), known as statistical physics, has been the way of solving large systems without having to solve an unreasonable amount of equations. Particularly, the notion of a statistical ensemble is at the head of this approach. This formalism is able to describe what is known as a phase transition, during which the properties of the system change, often discontinuously.

Blackouts and cascading outages are examples of collective behavior, that show signs of being phase transitions[10], in the power system that are governed by the system's structural, not thermal, properties in the sense that transmission line and network node outages change the network topology and operations. This is seemingly at odds with the thermodynamic foundation of ensembles in statistical mechanics. Regardless of this divide, can a statistical mechanical approach yield insights into blackouts and cascading outages?

As has been mentioned, physicists have already made contributions in this space through studies of complex network and dynamical models. Is a statistical mechanical approach able to produce the same results? Can it produce new results?

1.1 Objectives

The **main objective** of the master thesis is to investigate blackouts or cascading outages in power systems through the application of methods from statistical mechanics.

Intermediate objectives to accomplish this include

-Choosing a model that facilitates/enables a statistical mechanical treatment

-Identify suitable statistical mechanical method(s)

-Compare the results obtained to previous work

-Investigate the behavior of different network types and explain any differences

-Evaluate the viability of this approach

1.2 Scope

Explain in short the limitations of a statistical mechanical approach and the chosen model. What kind of phenomena will be modeled and what can be inferred by this.

In this thesis a simplified model of the power grid is considered. We model the angle interactions between network components and the dynamics of transmission line operations. The model is dynamical in nature, however dynamical simulations will not be performed. Instead we focus on studying the system using the canonical ensemble and Monte Carlo importance sampling from statistical mechanics. We consider very basic control schemes for operating the network and only small test systems will be studied.

1.3 Outline

What will be explained where. To begin with we will in chapter 2 introduce the theory that will be applied later on. This includes the power grid model, relevant topics from statistical mechanics and Monte Carlo importance sampling. In chapter 3, the tweaks and changes to the model will be introduced, together with the different network types that will be studied and also an explanation of the sampling algorithm. In chapter 4 we will make some general remarks about applying a thermal ensemble to a non-thermal system and results of the simulations will be presented and discussed. Finally, conclusions will be drawn and further work proposed in chapter 5.

Chapter 2

Theory

2.1 Power system model

The model which will be studied in this thesis is the one introduced by Yang & Motter [4], an extension of the swing equation [11] to include a continuous and dynamical state variable for each transmission line in the power grid.

In this model each line ℓ is associated with a continuous variable η_ℓ representing its on-off status and a parameter λ_ℓ indicating the fraction of the line capacity used by the flow. $\lambda_\ell < 1$ represents a normal operating state, while $\lambda_\ell \geq 1$ a failed operating state. The power flow terms of the swing equation are scaled by η_ℓ, thus constraining η_ℓ to the unit interval. This implies that when $\eta_\ell \approx 1$ the line is switched completely on, $\eta_\ell \approx 0$ the line is switched completely off. The dynamics of η_ℓ are then defined as

$$\dot{\eta}_\ell = f(\eta_\ell) - \lambda_\ell, \tag{2.1}$$

where the choice of f, along with a few other conditions elaborated upon in [4], is such that the equation can be rewritten as a gradient system $\dot{\eta}_\ell = -d\phi(\eta_\ell)/d\eta_\ell$, where $\phi(\eta_\ell) = \lambda_\ell \eta_\ell - F(\eta_\ell)$, and $dF(\eta_\ell)/d\eta_\ell = f(\eta_\ell)$. As shown in Fig. 2.1 this choice of f results in a potential function with two stable minima when $\lambda_\ell < 1$, one for the line being on, one for the line being off. The potential function ϕ contains these two minima as λ_ℓ is increased until it reaches 1, at which point the line is overloaded and there no longer exists a stable minima for the line being on. As with a potential function in classical mechanics we then expect that its associated phase space coordinate η_ℓ will "roll" down the slope to reach a low value, indicating that the line has been switched off.

Having considered the line dynamics, we now look at the rest of the network. There are n_g generator nodes connected to the network through virtual lines (not subject to failure). Each generator is a rotating machine where power is injected into the system. In addition there are n nongenerator nodes. Each nongenerator includes some power exchange, and/or power distribution to other nodes in the network along transmission lines. This leads to a network of $n + n_g$ nodes. There are n_l transmission lines connecting such nongenerator nodes . Here we follow

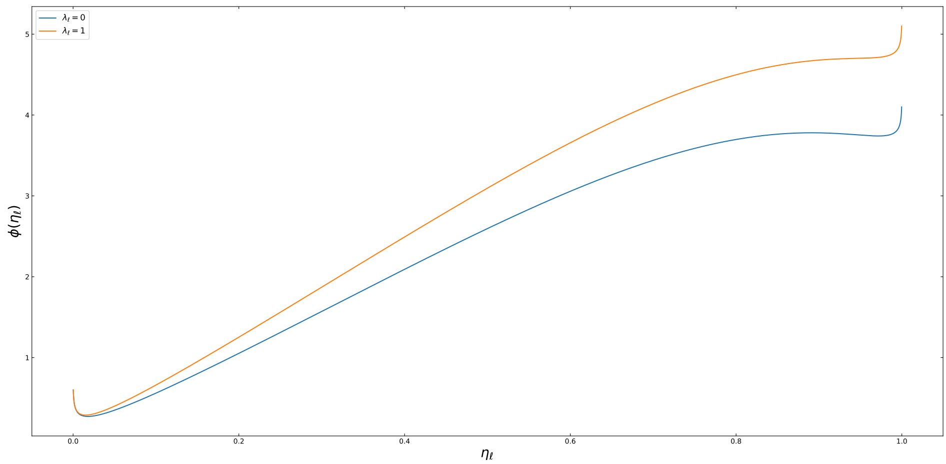

Figure 2.1: Plot of the transmission line potential $\phi(\eta_\ell)$ for two values of λ_ℓ.

the convention of the original authors and reindex the generators as the first n_g nodes. For convenience we also adopt the convention of referring to the generator nodes as generators and the nongenerator nodes as loads. Loads can also be pure transmission nodes.

The complex electrical power at node i is given by $S_i^{(e)} = P_i^{(e)} + \mathrm{j}Q_i^{(e)}$ where $P_i^{(e)}$ is the real, or active, power and $Q_i^{(e)}$ is the reactive power. The complex voltage at node i is given by $V_i = |V_i|e^{\mathrm{j}\delta_i}$, where δ_i is the voltage angle relative to a reference node(taken to be $i = 1$, so that $\delta_1 \equiv 0$). The power flow equations of a power-grid are given by:

$$P_i^{(e)} = \sum_{j=1}^{n_g+n} |V_i||V_j|(\tilde{G}_{ij}\cos\delta_{ij} + \tilde{B}_{ij}\sin\delta_{ij}), \tag{2.2}$$

$$Q_i^{(e)} = -\sum_{j=1}^{n_g+n} |V_i||V_j|(\tilde{G}_{ij}\sin\delta_{ij} - \tilde{B}_{ij}\cos\delta_{ij}), \tag{2.3}$$

where $\delta_{ij} = \delta_i - \delta_j$, $\tilde{Y}_{ij} = \tilde{G}_{ij} + \mathrm{j}\tilde{B}_{ij}$ is the nodal admittance matrix where each off-diagonal element $\tilde{Y}_{ij}$ is the negative of the admittance of the line connecting node i and j.

We use the DC approximation [12] in which we assume that the voltages are equal everywhere and employ the per unit system [13] so that $|V_i| = |V_j| = 1$p.u.. In the DC approximation we also assume that $\tilde{G}_{ij} = 0$, which is equivalent to saying that there is no real power lost on the transmission lines. These are well-known assumptions about power systems that are often applied to simplify the description of the system [14]. This leads to the expression for the real power at node i:

$$P_i^{(e)} = \sum_{j=1}^{n_g+n} \tilde{B}_{ij} \sin{(\delta_i - \delta_j)}, \tag{2.4}$$

where $\tilde{B}_{ij} = -1/x_{\ell_{ij}}$ with $x_{\ell_{ij}}$ being the transient reactance of the generator or the reactance of the transmission line, depending on whether the line between nodes i and j is virtual or not. Since power flows from leading angle to lagging angle we get $P_i^{(e)} > 0$ at a node where power is drawn out of the system while we get $P_i^{(e)} < 0$ when power is injected into the system at node i.

The state of the power system can be compactly defined as $\mathbf{x} = (\boldsymbol{\omega}, \boldsymbol{\delta}, \boldsymbol{\eta})$. Here, $\boldsymbol{\omega} = (\omega_i)$ are the frequencies of the generators relative to the systems nominal frequency, $\boldsymbol{\delta} = (\delta_i)$ are the voltage angles, and $\boldsymbol{\eta} = (\eta_\ell)$ are the status variables of the (nonvirtual) transmission lines $\mathcal{L}$, where $\ell \in \mathcal{L}$. We now state the equations of motion of the system. A complete derivation can be found in [4].

$$\begin{aligned}
\dot{\omega_i} &= -\frac{D_i}{M_i}\omega_i - \frac{1}{M_i}\left(P_i - \sum_{j=n_g+1}^{n_g+n} \tilde{B}_{ij} \sin \delta_{ij}\right), && i = 1, 2, ..., n_g, \\
\dot{\delta_i} &= \omega_i - \omega_1, && i = 2, ..., n_g, \\
\dot{\delta_i} &= -\frac{1}{T_i}\left(P_i - \sum_{j=1}^{n_g} \tilde{B}_{ij} \sin \delta_{ij} - \sum_{j=n_g+1}^{n_g+n} \tilde{B}_{ij} \eta_{\ell_{ij}} \sin \delta_{ij}\right) - \omega_1, && i = n_g{+}1, ..., n_g{+}n, \\
\dot{\eta_{\ell_{ij}}} &= 10\left(f(\eta_{\ell_{ij}}) + \frac{\tilde{B}_{ij}(1 - \cos \delta_{ij})}{W_{\ell_{ij}}}\right), && \ell_{ij} \in \mathcal{L}.
\end{aligned} \tag{2.5}$$

The first two equations describe the dynamics of the generators, with M_i being the rotor inertia, D_i being the damping ratio and P_i being the negative of the power input $P_i^{(m)}$. The third equation describes the dynamics of the loads, with T_i being the load frequency radio and P_i being the power $P_i^{(d)}$ demanded at the load. It is assumed that $\sum_{i=1}^{n+n_g} P_i = 0$. The last equation is Eq. 2.1 with λ_ℓ being replaced by $\tilde{B}_{ij}(1 - \cos \delta_{ij})$, the reactance energy stored on transmission line ℓ_{ij}, divided by $W_{\ell_{ij}}$, the line's maximum capacity. The prefactor 10 makes sure that the time scale for changes in $\eta_{\ell_{ij}}$ is shorter than that of the other variables.

It can be shown that Eq. 2.5 can be derived from a Hamiltonian-like system of the form

$$\dot{\mathbf{x}} = J \nabla \Psi(\mathbf{x}), \tag{2.6}$$

where the matrix J can be found in [4] and $\Psi(\mathbf{x})$ is an energy function defined as

$$\Psi(\mathbf{x}) = \sum_{i=1}^{n_g} \left[\frac{1}{2} M_i \omega_i^2 - \sum_{j=n_g+1}^{n_g+n} \tilde{B}_{ij}(1 - \cos\delta_{ij}) \right] - \sum_{i=n_g+1}^{n_g+n} \sum_{j=i+1}^{n_g+n} \tilde{B}_{ij}(1-\cos\delta_{ij})\eta_{\ell_{ij}} + \sum_{i=2}^{n_g+n} P_i\delta_i - \sum_{\ell_{ij}\in\mathcal{L}} W_{\ell_{ij}} F(\eta_{\ell_{ij}}). \tag{2.7}$$

We rewrite this as

$$\Psi(\mathbf{x}) = \Psi_{generator} + \Psi_{generator-load} + \Psi_{load-load} + \Psi_{load} + \Psi_{line}, \tag{2.8}$$

with

$$\Psi_{generator} = \sum_{i=1}^{n_g} \frac{1}{2} M_i\omega_i^2 + P_i\delta_i, \quad \Psi_{generator-load} = -\sum_{i=1}^{n_g} \sum_{j=n_g+1}^{n_g+n} \tilde{B}_{ij}(1-\cos\delta_{ij}),$$

$$\Psi_{load-load} = -\sum_{i=n_g+1}^{n_g+n} \sum_{j=i+1}^{n_g+n} \tilde{B}_{ij}(1-\cos\delta_{ij})\eta_{\ell_{ij}}, \quad \Psi_{load} = \sum_{i=n_g+1}^{n_g+n} P_i\delta_i,$$

$$\Psi_{line} = -\sum_{\ell_{ij}\in\mathcal{L}} W_{\ell_{ij}} F(\eta_{\ell_{ij}}).$$

We can then provide an interpretation for all the terms in the energy function: $\Psi_{generator}$ is the rotational energy stored in the generators plus a term where the power input acts as a linear field that interacts with the generators' δ_i.
$\Psi_{generator-load}$ can be identified as the reactance energy stored on the virtual lines between generators and loads. $\Psi_{load-load}$ is the reactance energy stored on the transmission lines between loads. Ψ_{load} is the power demand interacting with δ_i of the loads. Ψ_{line} does not have an interpretation on its own, but the combination $\Psi_{load-load} + \Psi_{line} = \sum_{\ell_{ij}\in\mathcal{L}} W_{\ell_{ij}}\phi(\eta_{\ell_{ij}})$ is the sum of each transmission line's potential multiplied by its capacity.

2.2 Statistical Mechanics

Statistical Mechanics is a field that is concerned with deriving the macroscopic behavior of a system starting out from knowledge about its microscopic behavior. By macroscopic we mean a system of many constituents, as opposed to a microscopic system, one of few constituents. In the microscopic case, by behavior we mean the behavior of each constituent, in general its position, momentum and interaction with other constituents or boundaries. In the macroscopic case, behavior is meant to denote the properties of the system emerging from its constituents. Examples include pressure, volume, thermal properties and existence and properties of different phases of matter. The notion of a *phase* will be introduced shortly.

In general, the motivation for a statistical mechanical treatment is threefold. Solving equations of motion becomes computationally (by hand and otherwise) unfeasible for large systems. The insight gained from solving the system exactly would not be much better than a statistical approach, thereby hardly justifying the time and space (in bytes) required to obtain and store it. Thirdly, for a chaotic system the detailed solutions and whatever we infer from them would, in large part, be meaningless [15].

2.2.1 Canonical ensemble

An important concept of Statistical Mechanics is the canonical ensemble. It is a collection of identical copies of a system described by an energy function, connected to a heat bath. The distribution of energies of the copies has the following form:

$$P(E_j) = \frac{e^{-\beta E_j}}{Z}, \tag{2.9}$$

where $\beta = \frac{1}{k_b T}$, k_b is the Boltzmann constant and T is the temperature of the heat bath, E_j is the energy of a state j and Z is the canonical partition function defined by

$$Z = \sum_j e^{-\beta E_j}. \tag{2.10}$$

According to 2.9, by randomly selecting a system from the ensemble, it is more likely to have lower energy than higher. To calculate the ensemble average of some property X one simply has to calculate

$$\langle X \rangle = \sum_j X_j P(E_j) = \frac{1}{Z} \sum_j X_j e^{-\beta E_j}. \tag{2.11}$$

Often times this equation is difficult to solve. This is especially the case for higher dimension problems, to the point where it might be impossible and other avenues must be taken to obtain an answer.

Earlier the concept of the system's boundary was mentioned. Its role in the canonical ensemble deserves to be explained. A boundary is simply the system's interface with the outside world. For a gas of particles in a container the boundary would be the walls of the container, where particles colliding with the wall can exchange energy with the outside world. The boundary can also come in the form of a field, say gravitational, electric or magnetic. Depending on the system, these interactions with its boundaries may or may not be modeled explicitly in the Hamiltonian. An important detail in the derivation of the canonical ensemble is that we let the systems in the ensemble exchange energy with each other. This energy exchange is mediated by heat transfer at the physical boundaries, making no claims as to the actual physical mechanism that enables the exchange. Returning to the ideal gas then, by applying the canonical ensemble to this system we are introducing energy exchange to the model and the results must be interpreted with this in mind. For example, if there exists no conceivable mechanism for this energy exchange the results are probably meaningless. For the ideal gas though, we can conceive that phonons are absorbed by the gas particles as they collide with the walls of the container, or perhaps they absorb radiation emitted by the walls.

2.3 Monte Carlo importance sampling

Monte Carlo (MC) methods denote methods that make use of random numbers to obtain numerical results of problems, such as integrals or sampling a probability distribution. Here we will consider MC importance sampling.

We are interested in obtaining some information about the power system such as average quantities in Eq. 2.11. An important observation in this regard is that the number of system configurations to consider are too many to be able to consider them all within a reasonable time frame, especially for larger systems. Additionally, in performing the calculation of 2.11, a potentially large part of the possible system configurations have small or virtually no contributions to the sum. The challenge is then to carefully consider as few configurations as possible while still making sure that the average 2.11 becomes as precise as possible. This is exactly what MC importance sampling seeks to do. In this thesis the Metropolis scheme as outlined in [16] will be adopted. In this scheme we generate configurations from a previous state using transition probabilities. These transition probabilities depend on the energy difference between the initial and final states. We produce a 'Monte Carlo time' ordered chain of states that is not deterministic in the way that an ordered sequence of states generated from the equations of motion would be. This is due to the sampling of states using random numbers.

We start with the MC time-dependent behavior which in equilibrium must obey what is known as detailed balance

$$P_n(t)W_{n\to m} = P_m(t)W_{m\to n}, \tag{2.12}$$

where $P_n(t)$ is the probability of the system being in state n at MC time t, and $W_{n\to m}$ is the transition rate for $n \to m$. What this means is that in our canonical ensemble the number of copies in each state stays constant.

We must now construct transition rates that satisfy Eq. 2.12. We do this by splitting up the transition into two steps. In the first step we suggest a new state m given the state n. In the second we decide whether we accept or reject the suggestion. This can be expressed by $W_{n\to m} = G_{n\to m}A_{n\to m}$, where $G_{n\to m}$ is the symmetrical probability of suggesting state m given state n and $A_{n\to m}$, the probability to accept state m given state n. Eq. 2.12 then becomes

$$\frac{A_{m\to n}}{A_{n\to m}} = \frac{P_m G_{m\to n}}{P_n G_{n\to m}} \tag{2.13}$$

The Metropolis choice is

$$A_{n\to m} = min\left(1, \frac{P_m G_{n\to m}}{P_n G_{m\to n}}\right), \tag{2.14}$$

for which Eq. 2.13 is satisfied.

According to 2.9 the probability of the nth state occurring in our system is given by

$$P_n = e^{-\beta E_n}/Z, \tag{2.15}$$

where Z is the partition function. We can now outline the Metropolis importance sampling Monte Carlo scheme:

1. Select an initial state.
2. Consider the first state variable.
3. Suggest the next state using $G_{n\to m}$.
4. Calculate the energy difference $\Delta E = E_n - E_m$ between the two states.
5. Generate a random number $r \in [0, 1]$. Note that r must be drawn uniformly from the interval.
6. If $r \leq exp(-\beta\Delta E)$, accept the new state. Otherwise, leave the variable unchanged.
7. Consider the next state variable and go to 3.

A consequence of this choice of transition rate is that the resulting Markov Chain has its states distributed according to Eq. 2.15. This has the convenient consequence that the ensemble averages in Eq. 2.11 become arithmetic averages over the entire sample of states which are generated. That is to say: let $\{\mathbf{x}_0, ..., \mathbf{x}_T\}$ be the set of states saved in the Markov Chain of length T. Then the averages become

$$\langle A\rangle = \sum_j A_j P(E_j) = \frac{1}{Z}\sum_j A_j e^{-\beta E_j} = \frac{1}{T}\sum_{i=1}^{T} A_i. \tag{2.16}$$

In general we require the algorithm to conduct a certain number of steps before we start recording the states. This is called thermalization, and is done to make sure the system has reached equilibrium before we start recording. If we are not mindful of this we risk not getting the desired distribution.

Chapter 3

Method

3.1 Adjustments of the model

3.1.1 Capacity scaling

Each transmission line η_ℓ in the network has a maximum capacity $W_{\eta_{\ell_{ij}}}$. To be able to have an extra way of tuning the system we have scaled all these capacities by a common factor K so that

$$W_{\eta_{\ell_{ij}}} \to KW_{\eta_{\ell_{ij}}}. \tag{3.1}$$

3.1.2 Corrective actions

During simulations we must make sure that every sample of the network is consistent and physically realizable. Power must be balanced and proper corrective actions must be taken in case the network is disturbed. The corrective actions included in this thesis are the following ones.

Islanding, which is the condition in which the system has split into different unconnected subsystems (islands). Not allowing the system to operate in this condition implies that any island other than the one with the original reference generator loses its generation and load. In this thesis, islanding is allowed so that when the network is split, each new island has its generator with the lowest index assigned as the new reference generator. In this process the angles of all other nodes in this island must be recalculated to be relative to the new reference generator. The angle of the new reference generator will continue to be sampled, so that it can be reset to the new reference frame in the case that the island merges with another one.

Load/generation shedding is the act of reducing the amount of load or generation in the system. In the model it is a requirement that power is balanced in every island. Thus, for each island, the algorithm will identify whether there is power balance, and in the case of an imbalance, will distribute the *slack* proportional to each generator/node's capacity.

These corrective actions are among those that have the most impact on the network reliability [17]. This modeling of corrective actions is optimistic and results in a more realistic model than the case where these are excluded.

3.1.3 Frequency assumptions

As we can see in Eq. 2.7 the energy function contains a frequency term. The power supplied by the generators does also vary slightly with the frequency [4]. It is however assumed that the frequencies are much smaller than the reference frequency of the network [4] so that these variations are negligible. The frequency-angle coupling would then be dominated by the quadratic potential, which simply averages to zero, something that isn't particularly interesting. Additionally, we must consider that the extra computational complexity introduced by this frequency-dependent power injection is significant, particularly for larger systems, seeing as we would have to implement corrective actions related to slack [17]. Therefore, we have omitted the frequencies completely.

3.1.4 Alternative f

As we know, the system energy function in Eq. 2.7 contains the potential function for the η_ℓ variables. This potential function is introduced in [4] as a means of obtaining a time-continuous model of the state of a transmission line. The requirements are that it contains stable equilibria for the normal and failed operating status when the line is operating below capacity($\lambda_\ell < 1$), a stable equilibrium only for the failed operating status when the line is overloaded($\lambda_\ell \geq 1$) and that the equilibrium for normal operating status is close to 1 and the failed operating status is close to 0. As long as one satisfies these requirements one is generally free to suggest any other function f. Any new suggested f can simply replace the old one in 2.5 and its antiderivative F will in any case be present in the energy function, as long as it is only a function of η_ℓ.

A motivation for introducing an alternative F and hence ϕ is that the one suggested in [4] and shown in Fig. 2.1 is primarily constructed for dynamical simulations. If we start a dynamical simulation of the system with line η_ℓ being on, it will stay that way until the line is overloaded after which η_ℓ moves towards 0. As long as $\lambda_\ell < 1$ it does not really matter that the energy for the failed state is lower than the normal state. η_ℓ will move around in the basin close to 1. As soon as the line is overloaded(λ_ℓ) however, the energy for the failed state must be the only equilibrium point and located close to 0 to guarantee a line switch-off operation. The shape of the potential between the failed and normal operating states is also not very important, as long as it does not hinder a line switch-off operation. In a statistical mechanical treatment this form for the transmission line potential is not very intuitive. We expect that for high β (low T) the power system stays close to its normal operating state. That means all lines turned on. However, we know that in the canonical ensemble at low temperatures we only get contributions from the states with the lowest energy. In this case this has the unfortunate consequence that all lines are switched off. Perhaps a different choice of F then can bring

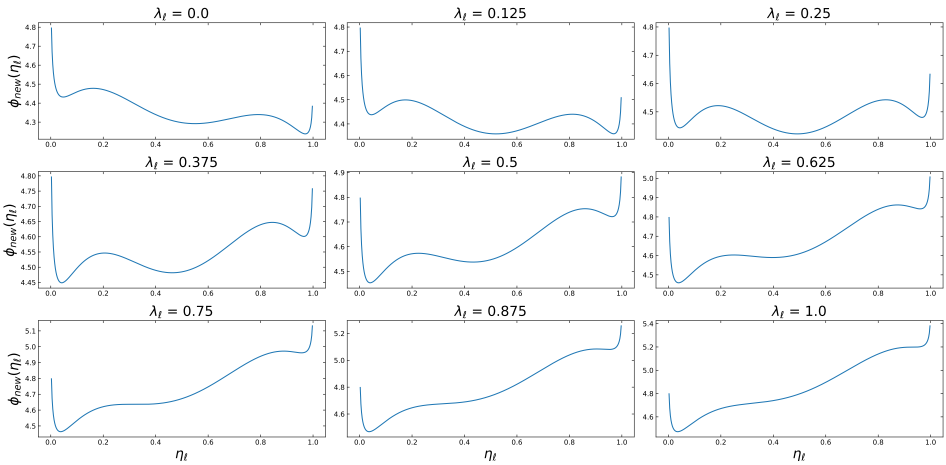

Figure 3.1: ϕ_{new} for different values of λ.

about more meaningful results, while keeping the model practically unchanged. We propose the following F:

$$F_{new}(\eta_\ell) = -F(\eta_\ell) - (1.01 - \eta_\ell)F(1 - \eta_\ell). \tag{3.2}$$

This leads to a new ϕ_{new}:

$$\phi_{new}(\eta_\ell) = \lambda_\ell \eta_\ell - F(\eta_\ell) - (1.01 - \eta_\ell)F(1 - \eta_\ell), \tag{3.3}$$

which is shown for different values of λ_ℓ in Fig. 3.1. Here we observe a more intuitive potential function. We have kept the properties of the original one. For $\lambda_\ell < 1$ there is a stable minimum for high η_ℓ and for $\lambda_\ell \geq 1$ there is only one stable equilibrium, which is positioned at low η_ℓ. In addition to this the resulting potential function displays a global minimum in the normal operating state(high η_ℓ) for low λ_ℓ which facilitates the interpretation of statistical mechanical simulations.

This raises a question. Do our results carry any meaning, if they can so easily be manipulated? It is indeed interesting that such different potential functions can give rise to the same dynamics.

3.2 Network data and parameters

The system parameters used in this thesis are taken from or loosely based on [14], since it studies small test systems whose parameters are tuned to resemble the real power system.

We will study two test systems that are small, where each one distinctly displays different mechanisms of the model and method.

The first test system, shown in Fig. 3.2, is a network consisting of a single generator and single load. Since generators are connected to the network through

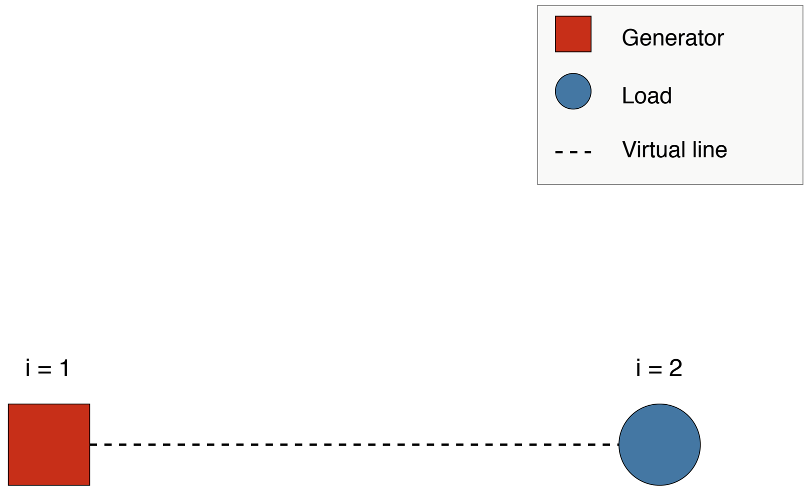

Figure 3.2: Schematic of the generator-load system.

Variable	Explanation	Value
P_1	Generator 1 power	1
P_2	Load 2 power	-1
$x_{\ell_{12}}$	Transient reactance generator 1	1/242

Table 3.1: Parameters for the generator-load system.

a virtual line, this system does not contain any line dynamics, thereby isolating the behavior of the angles and without any disturbance. The parameters are given in Table 3.1.

The second test system, shown in Fig. 3.3, is a network consisting of two generator-load pairs connected through a transmission line. This system incorporates the mechanism of islanding through the removable transmission line. By creating a mismatch between power generation and consumption on each ”side” of the transmission line one can increase the power flow between the ”sides”, letting us stress the system in more than one way and study the consequences. We will consider two versions of this system. One version with a balance of power between the sides, and one version where there is an imbalance of power. The parameters for these versions are given in Table 3.2.

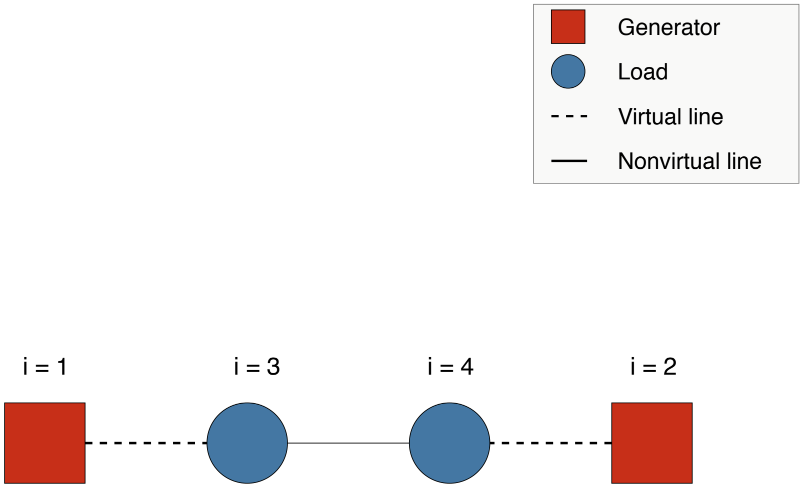

Figure 3.3: Schematic of the radial system.

Variable	Explanation	Value
$P_1^{(b)}$	Generator 1 power	-0.5
$P_2^{(b)}$	Generator 2 power	-0.5
$P_3^{(b)}$	Load 3 power	0.5
$P_4^{(b)}$	Load 4 power	0.5
$P_1^{(i)}$	Generator 1 power	-0.9
$P_2^{(i)}$	Generator 2 power	-0.1
$P_3^{(i)}$	Load 3 power	0.1
$P_4^{(i)}$	Load 4 power	0.9
$x_{\ell_{13}}$	Transient reactance generator 1	1/242
$x_{\ell_{24}}$	Transient reactance generator 2	1/242
$x_{\ell_{34}}$	Reactance between node 3 and 4	5
$W_{\ell_{34}}$	Maxiumum reactance energy line ℓ_{34} can hold	1/5

Table 3.2: Parameters for the radial system. Superscript b denotes the system with power balance and superscript i denotes the system with power imbalance.

3.3 Monte Carlo method

Here the choices of suggestion function will be presented. We will also look at the different observables that we will measure.

3.3.1 Suggestion function

Specific choices of sampling and their justifications. For the angles we have chosen to suggest new states in the following way: consider the previous state's angle δ_i. The suggestion for a new angle is then simply a slight perturbation:

$$\delta_i \rightarrow \delta_i + \Theta_r, \tag{3.4}$$

where Θ_r is an angle uniformly drawn from the interval $[-\frac{\pi}{6}, \frac{\pi}{6}]$.

For the line state variables we have considered the same scheme as for the angles, however it turns out that this scheme produces the same results as sampling uniformly from the unit interval. Due to ease of implementation we have chosen a uniform sampling from the unit interval.

3.3.2 Observables

For these small systems we have chosen to look at the behavior of the state variables δ_i and $\eta_{\ell_{ij}}$ because we want to focus on understanding how this model is suited to a statistical mechanical approach. To study correlations, particularly among transmission lines, we would have to consider larger systems.

Chapter 4

Results and discussion

We start with a discussion on applying the canonical ensemble to our non-thermal system. Then we proceed with presenting and discussing results from simulations.

4.1 Non-thermal systems

The model previously introduced in section 2.1, while every bit as mechanical as a collection of particles, is not thermal in the sense that one could heat it up and observe a change in its properties as one can with a gas. Granted, while the components would surely have some temperature-dependent behavior had they been implemented in a laboratory, it remains that the rotating machines would not be sped up had we heated the room. One might then question how one can, and why one would, study such a model using a framework developed for studying thermal systems. Furthermore, if temperature is not defined for our system, can we give some other interpretation of the β in equation 2.9?

Complex systems denote systems that are difficult to model due to complex relationships. The power system can be considered to be complex. Complex systems are in general united by the absence of concepts such as temperature and energy, display behavior governed by stochastic laws of non-thermodynamic nature and can be called non-thermal [18]. Nevertheless, we know that due to non-thermal fluctuations the behavior of complex systems resembles the behavior of thermodynamic systems [18]. This has led researchers to attempt to generalize the formalism of statistical physics so that it would become applicable for non-thermal systems [18]. Examples in the complex network space include introducing ”energies” with different types of interactions between components [8, 9] and the application of the Ising model to analyze the spread of rumors in networked social communities [19].

The power grid model in 2.1 has energy as an integral part to it. Real energy is flowing between real rotating machines. Furthermore, there is even an energy function (2.7) that governs some of the dynamics and network topology. This energy function is what enables a statistical mechanical approach, provided that we are careful in the process by keeping the thermal and non-thermal nature of the

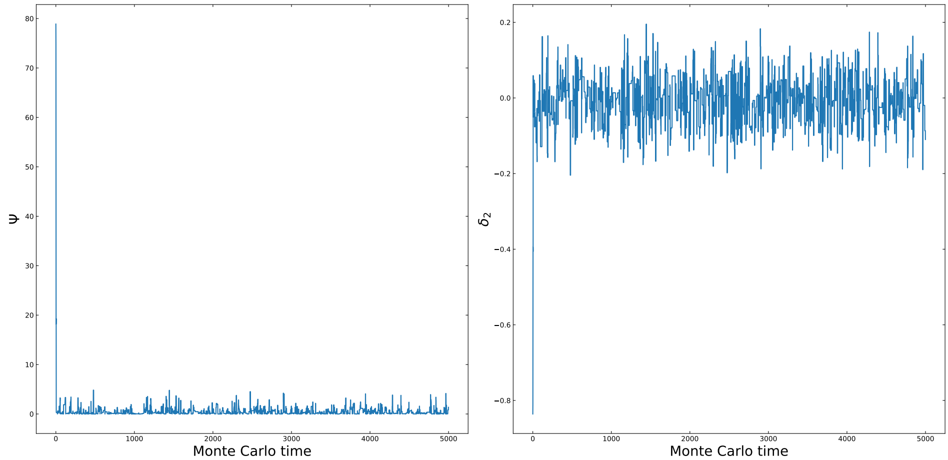

Figure 4.1: The evolution of the system during a sample run with $\beta = 1$.

system in mind.

In our model of the power system we are assuming that fluctuations exist. These fluctuations are thermal in the sense that ultimately it is the energy flowing on transmission lines that is fluctuating. At the same time they are non-thermal in the sense that they are not thermally induced. There is no temperature that can define the likelihood of energy transfer at the system boundary. We must therefore seek to provide an interpretation of what the temperature T represents in our canonical ensemble.

4.2 Generator-load system

In Fig. 4.1 we observe the evolution of the system during a simulation. The steps required to reach equilibrium are very few, usually around 2-3 steps. After reaching equilibrium we observe the expected fluctuations around the equilibrium value of $\delta_2 = 0.0041$.

Next we investigate how long a simulation should be run for to get an acceptable distribution of angles. This is shown in Fig. 4.2 where we observe improved distributions as we increase the length of simulation. There seems to be a good trade off between simulation time and getting good distributions when doing around $500000 - 1000000$ MC steps. Of course, this should be evaluated for larger systems also, but this gives a good initial guess. Particularly for generators and loads connected to generators due to their high coupling $\tilde{B}_{ij}$ and tendency to dominate the load-load coupling terms.

In Fig. 4.3 we see the distribution of power at node 2. The biggest surprise here is that in a large part of the configurations power is actually flowing from the load to the generator; their roles are exchanged. This resembles the procedure in [5] where different realizations of the network have their nodes randomly selected

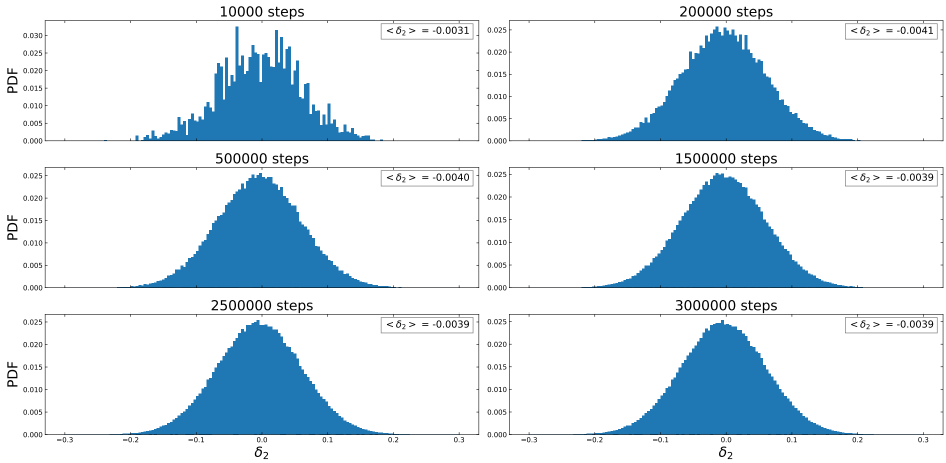

Figure 4.2: The probability density function(PDF) of δ_2 for different numbers of Monte Carlo steps with $\beta = 1$.

to either be power plants or consumers. At the same time the average power flow is in agreeance with the network parameter. Our method then, seems to embody the procedure where one stresses the system by letting power be generated and consumed everywhere as in [5] while still retaining information about the original or intended configuration.

We also observe huge variations in the amount of power flowing between the two nodes. As we will see shortly, this can be controlled by tuning β, but it is also due to the large value of $\tilde{B}_{ij}$ on the virtual lines. As the system evolves according to the equations of motion a high $\tilde{B}_{ij}$ guarantees a small angle difference (and hence instability) between the generator and nongenerator [4]. This is a favourable characteristic if one wants to study other parts of the network's response to disturbances. Energetically speaking however, there is nothing hindering larger angle differences and we observe that these states are reached in a statistical mechanical treatment.

In Fig. 4.4 we see how the power distribution varies with β. First of all we can see that the fluctuations in power decrease as we increase β. Here we can draw on our knowledge from thermal systems where in the case of a high β (low T) there is little energy available to the system, leading to small fluctuations in energy which is exactly what we observe. Conversely a low β (high T) should give rise to large fluctuations which we also observe. This provides us with an interpretation of β in this ensemble. It is simply a measure of how large the fluctuations in injected power at the system boundaries are. Put in other words: β is a measure of how much the power production/demand fluctuates. This behavior is also analogous to thermal systems where at low β (high T) there is a lot of energy available resulting in large energy fluctuations in the system.

We also see that as we increase β the distribution of power more closely resem-

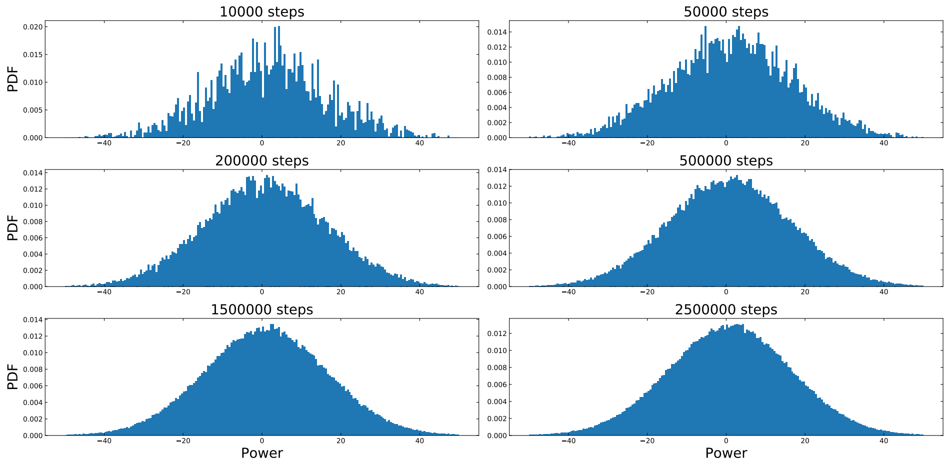

Figure 4.3: PDF of P_2 for different numbers of Monte Carlo steps with $\beta = 1$.

bles what we would expect from a dynamical simulation of the system. We can then state that as β increases the power system in the canonical ensemble deviates less and less from its dynamically simulated counterpart. This view coincides with the interpretation of β in [9]. There β measures the deviation of the network in the canonical ensemble from Erdös-Rényi networks, that is purely random networks, and in the case where $\beta \to \inf$ optimized networks are obtained. The most optimized version of our network is... our network. The most random version of our network is indeed what we see for low β.

4.3 Radial system

4.3.1 f

Plots: evolution, In Fig. 4.5 we see the MC evolution of the radial system with the original f. We observe that also here the system thermalizes very fast. Also note that δ_2 drops to zero immediately, which is the result of the network splitting into two islands and generator 2 becoming a reference generator. Apart from that we observe the expected fluctuations in the other variables.

In Fig. 4.6 we see the power flowing on the transmission line between loads 3 and 4. This power flow is of a magnitude we expect. We observe that the average of the power flow is close to or practically 0, which we also expect considering that there is a power balance between the two sides. We also see in the plot for $\beta = 0.1$ that there are two bumps in the PDF at the edges. This is due to the fact that these values of power are the maximum power than can flow on this line, given by the max of Eq. 2.4 which is $-\tilde{B}_{34} = 0.2$.

In Fig. 4.7 we again observe the power flowing between loads 3 and 4, however this for the imbalanced system. Compared to the balanced system we see that

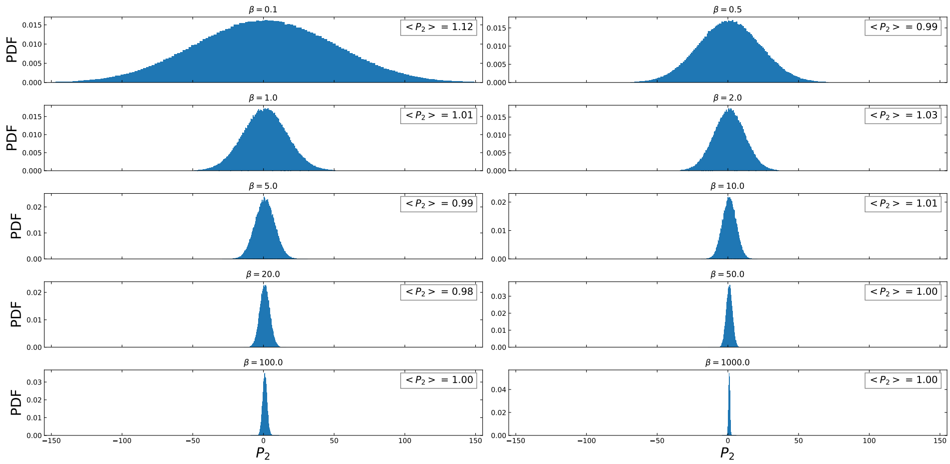

Figure 4.4: PDF of P_2 for different values of β, and 3000000 Monte Carlo steps.

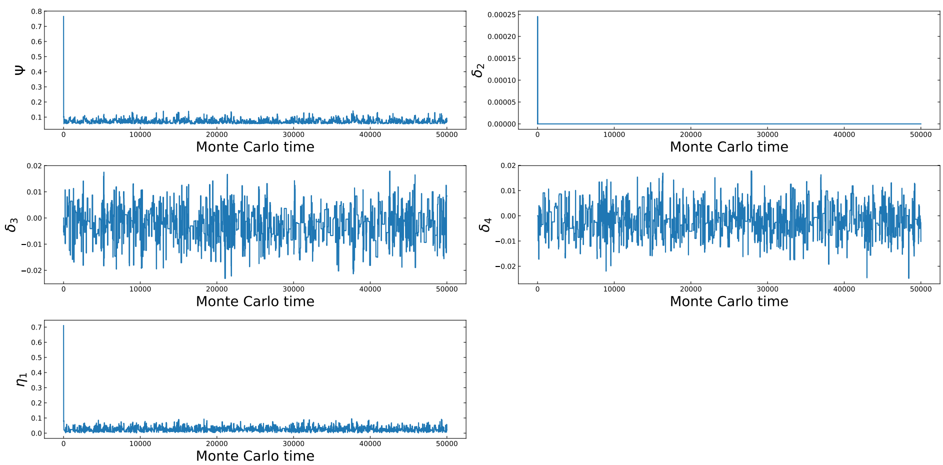

Figure 4.5: The first 50000 steps in a MC simulation of a balanced system with $K = \beta = 1$

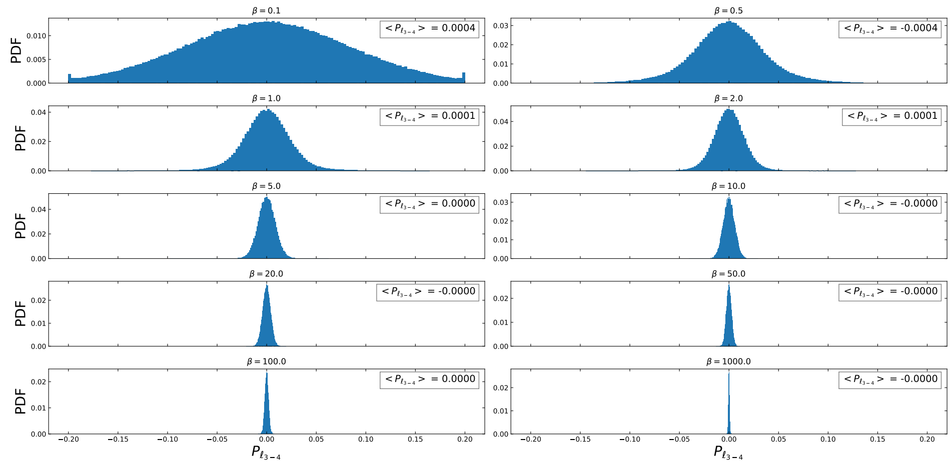

Figure 4.6: Distributions of power flow on line $\eta_{\ell_{34}}$ for a run of 1000000 steps and varying β. The system was balanced, $K = 1$ and the original F was used.

there flows more power, however this is only true for low values of $beta$. This is an unexpected result with no apparent explanation. In any case, we observe the same distributions and their dependence on β as we did for the generator-load system.

In Fig. 4.7 we observe that as β is increased the lines are turned off. This is sort of opposite to what we expect, but is an artifact of the f function. There is not much meaningful information to be extracted here.

Fig. 4.9 shows the averages of $\eta_{\ell_{34}}$ for the imbalanced system. It seems to be identical to the plot for the balanced system and equally hard to draw any meaningful information from.

4.3.2 f_{new}

We now consider the case where $F \to F_{new}$ given in Eq. 3.2. Consider Fig. 4.10 which shows $< \eta >$ for the balanced system. Here we get a more intuitive picture. Higher β now leads to a system that resides more often in its normal operating state. This is in line with what we expect to happen when the available energy decreases. We also see that it takes more and more energy to bring the system out of its normal operating state the higher its line capacities become. This is indicated by the steeper curves for higher K.

Looking at Fig. 4.11 which shows $< \eta >$ for the imbalanced system we see practically the same behavior. However we see that the curves do not go as high as in Fig. 4.10 for equal β. This is also expected, seeing as in general the power flow on the transmission line is higher, driving η a little further away from the normal operating state. We also observe a peculiar behavior for the $K = 10$ curve. This value for K probably leads to an average value for λ_ℓ where the form of F_{new} has a minimum that competes with the normal operating state. In Fig. 3.1 we see that

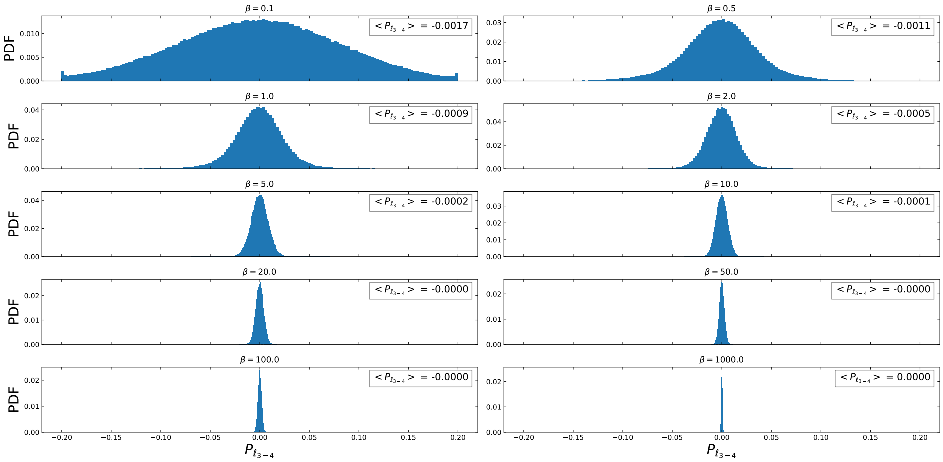

Figure 4.7: Distributions of power flow on line $\eta_{\ell_{34}}$ for a run of 1000000 steps and varying β. The system was imbalanced, $K = 1$ and the original F was used.

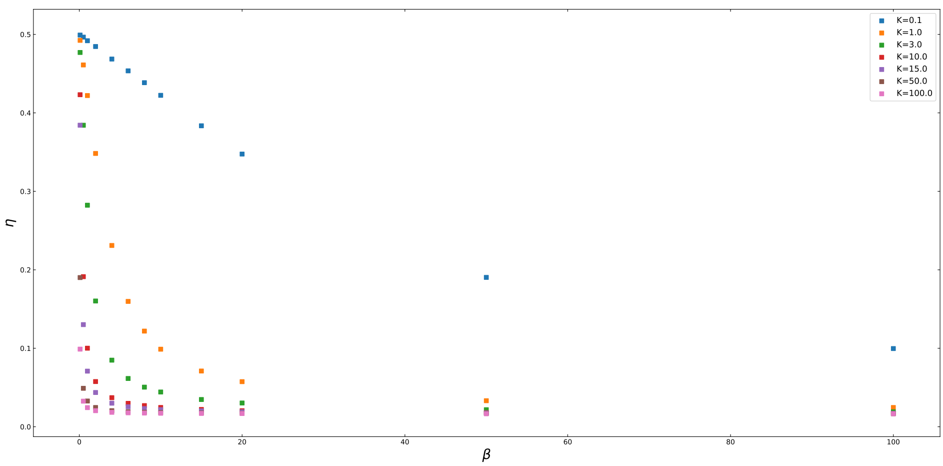

Figure 4.8: Plot of $< \eta_{\ell_{34}} >$ in the balanced radial system for varying β and K and the original function F. Each point is the average over a run of 500000 steps.

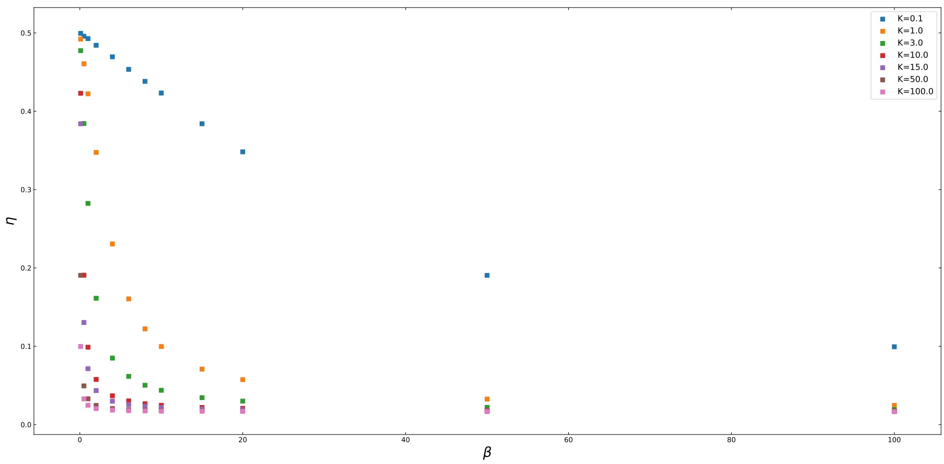

Figure 4.9: Plot of $< \eta_{\ell_{34}} >$ in the imbalanced radial system for varying β and K and the original function F. Each point is the average over a run of 500000 steps.

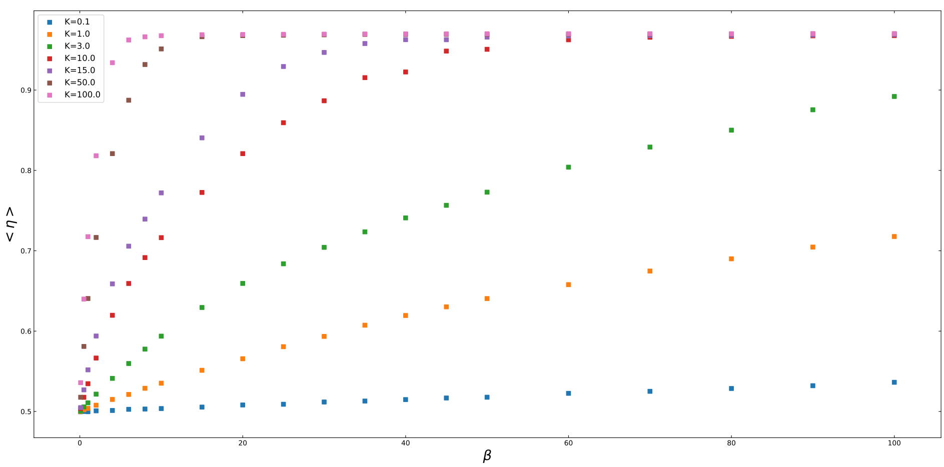

Figure 4.10: Plot of $< \eta_{\ell_{34}} >$ in the balanced radial system for varying β and K and the alternative function F_{new}. Each point is the average over a run of 500000 steps.

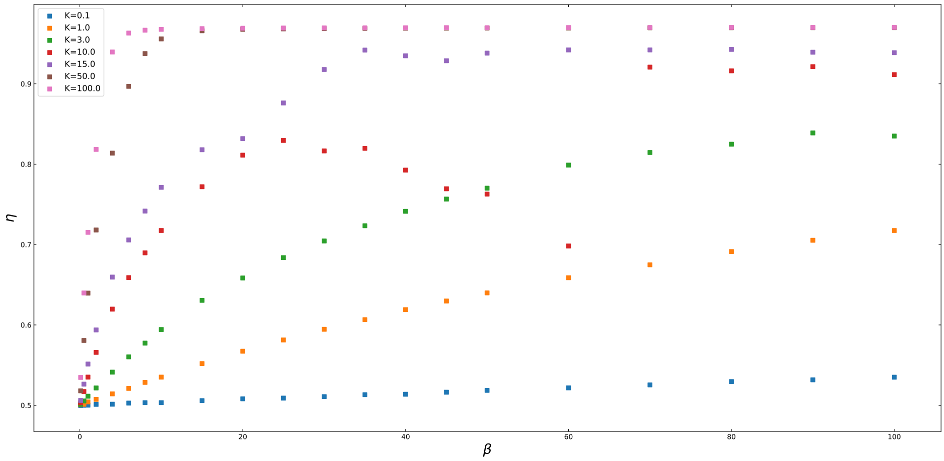

Figure 4.11: Plot of $< \eta_{\ell_{34}} >$ in the imbalanced radial system for varying β and K and the alternative function F_{new}. Each point is the average over a run of 500000 steps.

for $\lambda_\ell = 0.125$ this is exactly the case. We see it as an artifact of this potential function. Perhaps there are other choices for ϕ_{new} which don't have this behavior.

4.4 Viability of statistical mechanics approach

Discuss pros/cons of the kind of approach I have chosen. The statistical mechanics approach seems to provide results which are difficult to interpret. If we want to study blackouts and cascades then the most interesting variables are the on-off status variables η. The angles mainly play the role of driving the system in and out of normal and failed operating states. They are easy to interpret in that they simply fluctuate in their potential and through these fluctuations they impact the η potentials.

We have seen that the power flowing between generators and loads is orders of magnitude higher than the flow between loads, but this is an artifact of the low reactances between these nodes. This power only exists between the generators and loads and does not leak into the rest of the system. We could simply increase these reactances, but this would take us further away from the original model. We should not tweak the model only to please our eyes. The parameters should be set such that the model resembles the physical system as closely as possible.

Returning to the η, we have also seen how we can change its potential without changes to the dynamical behavior of the model, while bringing about changes in its behavior in the canonical ensemble.

An uplifting fact is also that the results we obtain do show differences between network types. Looking at the radial system we actually observe an average net power flow between the sides of the system. We also see a difference in the average of η with F_{new} between the balanced and imbalanced radial system.

All in all the statistical mechanics treatment does produce some strange results and is definitely not as straight forward to interpret as say a 1D Ising chain. On the other hand, there are a lot of meaningful and plausible results too, which could be studied further.

Chapter 5

Conclusions

In this thesis the power system has been studied using the canonical ensemble from statistical mechanics. To do this a model of the power system that can be described by a Hamiltonian-like energy function has been selected. This model includes the dynamics of the system frequencies, angles and transmission line time-continuous state variables. The frequencies were excluded from the problem and changes to the state variable potential function were proposed. This to make the energy function easier to interpret. Since the problem is difficult to solve analytically for large systems we employed Monte Carlo importance sampling to measure ensemble averages.

There are no previous accounts of studying such a detailed model of the power system using the canonical ensemble, so comparing the results to previous work mainly consisted of evaluating whether the results made sense compared to what has been obtained through dynamical simulations of similar models. And also comparing our interpretation of fluctuations and the role of β to their interpretations in other thermal and non-thermal systems.

In general it was hard to identify differences between different network types in the results, although there were some results that suggested that there are differences.

Finally we evaluated the viability of such an approach. The conclusion was that the results in general are hard to interpret, but do carry some meaning.

The main goal of the thesis was accomplished in the sense that information was gained about how the chosen model behaves in the canonical ensemble. Regrettably, larger systems have not been considered, so it is difficult to conclude that blackouts and cascades have been studied.

Further work could be the study of larger systems and therein the correlations between transmission lines. The role of f could also be studied further, since it seems like we are free to choose between different forms for it seemingly without affecting the behavior of the system. Does this imply that we can tailor our results to our liking based on a clever choice of f? Finally, employing other methods such as Kinetic Monte Carlo could be a viable approach, seeing as we have full information about the energy function of the system. This could be combined with knowledge obtained in this thesis regarding the distributions of power flows.

Bibliography

[1] Pagani GA, Aiello M. The Power Grid as a complex network: A survey. Physica A: Statistical Mechanics and its Applications. 2013;392(11):2688–2700.

[2] Cuadra L, Salcedo-Sanz S, Del Ser J, Jimnez-Fernndez S, Geem Z. A Critical Review of Robustness in Power Grids Using Complex Networks Concepts. Energies. 2015 Aug;8(9):92119265.

[3] Simonsen I, Buzna L, Peters K, Bornholdt S, Helbing D. Transient dynamics increasing network vulnerability to cascading failures. Physical review letters. 2008;100(21):218701.

[4] Yang Y, Motter AE. Cascading Failures as Continuous Phase-Space Transitions. Physical Review Letters. 2017;119(248302).

[5] Rohden M, Sorge A, Timme M, Witthaut D. Self-Organized Synchronization in Decentralized Power Grids. Physical Review Letters. 2012;109(064101).

[6] Schäfer B, Witthaut D, Timme M, Latora V. Dynamically induced cascading failures in power grids. Nature communications. 2018;9(1):1975.

[7] Albert R, Barabási AL. Statistical mechanics of complex networks. Reviews of modern physics. 2002;74(1):47.

[8] Palla G, Derenyi I, Farkas I, Vicsek T. Statistical mechanics of topological phase transitions in networks. Physical Review E. 2003;69(046117).

[9] Berg J, Lässig M. Correlated Random Networks. Physical Review Letters. 2002;89(228701).

[10] Dobson I, Carreras BA, Lynch VE, Newman DE. Complex systems analysis of series of blackouts: Cascading failure, critical points, and self-organization. Chaos: An Interdisciplinary Journal of Nonlinear Science. 2007;17(2):026103.

[11] Ulbig A, Borsche TS, Andersson G. Impact of Low Rotational Inertia on Power System Stability and Operation. In: 19th IFAC World Congress. Elsevier; 2014. p. 7290–7297.

[12] Purchala K, Meeus L, Van Dommelen D, Belmans R. Usefulness of DC power flow for active power flow analysis. In: IEEE Power Engineering Society General Meeting, 2005. IEEE; 2005. p. 454–459.

[13] Saadat H. Power System Analysis. PSA Publishing; 2010.

[14] Jakobsen SH, Uhlen K. Development of a test system for identification of turbine dynamics using the dc power flow. IFAC-PapersOnLine. 2018;51(2):97–102.

[15] Gould H, Tobochnik J. Statistical and Thermal Physics: With Computer Applications. Princeton University Press; 2010.

[16] Landau DP, Binder K. A Guide to Monte Carlo Simulations in Statistical Physics 2nd ed. Cambridge University Press; 2005.

[17] Sperstad IB, Jakobsen SH, Gjerde O. Modelling of corrective actions in power system reliability analysis. In: 2015 IEEE Eindhoven PowerTech. IEEE; 2015. p. 1–6.

[18] Abaimov SG. Statistical Physics of Non-Thermal Phase Transitions. Springer; 2015.

[19] Ostilli M, Yoneki E, Leung IXY, Mendes JFF, Li P, Crowcroft J. Statistical mechanics of rumour spreading in network communities. In: ICCS 2010. Elsevier; 2010. p. 2331–2339.

Appendix A

5.1 .json file format

Network data is input to the code as a .json file. This file format is easy to work with in the code itself, while also being easy to read and make changes to in most text/code editors. What follows is a description of the format.
n_g: number of generator nodes
n: number of nongenerator nodes
n_l: number of nonvirtual lines
line_index: zero-indexed and symmetric 2D array of dimension (n, n) where entry (i, j) is the index of nonvirtual line ℓ_{ij}. Only nongenerator nodes are included. For example entry $(0, 1)$ gives the index of the line between the first and second nongenerator nodes. If there is no line between node i and j entry (i, j) is 0. The line index is one-indexed.
index_to_lines: zero-indexed 2D array of dimension $(n\_l, 2)$ where the pair $[(i, 0), (i, 1)]$ are the two nodes connected by line i.
W: 1D array of length n_l containing the capacity of each line.
B: 2D array of dimension $(n\_g + n, n\_g + n)$ containing the transient reactances of the generators and reactances of the transmission lines.
P: 1D array of length $n\_g + n$ containing the per unit power inputs of the generator nodes and power demands of the nongenerator nodes.
initial_condition: 1D array of length $n\_g + n + n\_l$ containing the initial values for each variable of the system. The first n_g values are the generator angles, the next n values are the nongenerator angles and the last n_l values are the transmission line status.